

Comparison of Viscosity Models for the Simulation of Non-Newtonian Flow in Lid-Driven Cavity

Shreyas Shrestha¹, Tushar Chourushi², and Chandan Bose³

¹Aerospace Engineering, IOE, Pulchowk Campus, Tribhuvan University, Nepal

²Associate Professor, Department of Aerospace Engineering, MIT Art, Design and Technology University, Pune, Maharashtra 412201, India

³Assistant Professor, Aerospace Engineering, College of Engineering and Physical Sciences, The University of Birmingham, Birmingham B15 2TT, UK

September 11, 2025

Synopsis

This research migration project investigates transient simulations of the two-dimensional lid-driven cavity for non-Newtonian fluids using the open-source computational fluid dynamics (CFD) software OpenFOAM. The `nonNewtonianIcoFoam` solver, for incompressible, laminar, generalized Newtonian flow, is employed to assess the efficacy of four viscosity models: Power-law, Carreau, Carreau–Yasuda, and Casson. The velocity fields are validated against benchmark data from the literature using normalised velocity profiles along the cavity centerline. Simulations at $Re = 100$ and $Re = 400$ show that increasing the Reynolds number sharpens near-wall gradients and shifts the velocity peaks toward the walls. The migration uses reference datasets from Li *et al.* (Power-law) [1], Kim and Reddy (Carreau; Carreau–Yasuda) [2], and Neofytou (Casson) [3].

Keywords: Non-Newtonian fluids; Power-law fluids; Carreau model; Carreau–Yasuda model; Casson model; Lid-driven cavity; OpenFOAM.

1 Introduction

Non-Newtonian flows are prevalent in a wide range of materials and processes, from biological systems such as blood flow, to industrial applications in polymer manufacturing, adhesives, and paints, as well as consumer products like toothpaste, ketchup, mayonnaise, and shampoo [4]. Unlike Newtonian fluids, their viscosity varies with the shear rate and in some cases with time leading to behaviors such as shear-thinning, shear-thickening, and yield stress phenomena. Due to this, specific constitutive models and proper parameter selection are needed to analyze the flow accurately.

The lid-driven cavity is one of the most widely studied benchmark problems in computational fluid dynamics (CFD). It is a simple but useful way to learn about the basic flow physics. When applied to non-Newtonian fluids, it provides a useful framework for examining the impact of the viscosity-shear rate relationship on velocity profiles and vortex structures. OpenFOAM, which is an open source CFD software, offers dedicated solvers, like `nonNewtonianIcoFoam`, for simulating incompressible laminar flows of generalized Newtonian fluids. In this work, transient 2D lid-driven cavity flows are simulated using the Power-law, Carreau, Carreau–Yasuda, and Casson models, and the results are compared with velocity profiles reported in the literature.

2 Governing Equations and Models

2.1 Problem Definition

It consists of incompressible laminar flow inside a two-dimensional square domain of length 1 m in the x-y plane. The top wall has a constant velocity of 1 m/s in x-direction, while the other 3 walls are stationary. The fluid is non-Newtonian and is simulated using different viscosity models i.e. Power-law, Carreau, Carreau–Yasuda, and Casson model. The simulations are initially carried out for Reynolds number of 100 and later for 400, changing the lid velocity. The problem geometry is illustrated in Fig.1.

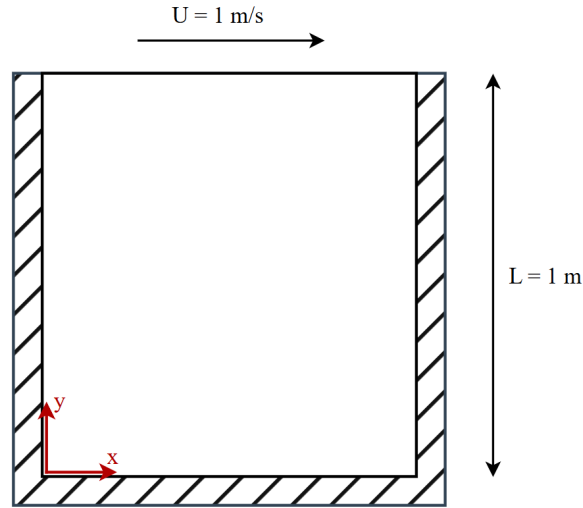


Figure 1: Problem geometry

2.2 Governing Equations

For incompressible, laminar, non-Newtonian flow, the governing equations are as follows:

2.2.1 Continuity equation

$$\nabla \cdot \mathbf{U} = 0 \quad (1)$$

where,

- $\mathbf{U} = (u, v)$ is the velocity vector field

2.2.2 Momentum equation

$$\frac{\partial \mathbf{U}}{\partial t} + \nabla \cdot (\mathbf{U}\mathbf{U}) = -\nabla p + \nabla \cdot \left[\nu(\dot{\gamma}) \left(\nabla \mathbf{U} + (\nabla \mathbf{U})^T \right) \right] \quad (2)$$

where,

- p is the kinematic pressure
- $\nu(\dot{\gamma})$ is the effective kinematic viscosity
- $\dot{\gamma} = \sqrt{2 \mathbf{D} : \mathbf{D}}$ is the magnitude of the shear rate
- $\mathbf{D} = \frac{1}{2}(\nabla \mathbf{U} + \nabla \mathbf{U}^T)$ is the rate-of-strain tensor

2.2.3 Viscosity models

The effective kinematic viscosity $\nu(\dot{\gamma})$ in `nonNewtonianIcoFoam` is computed from the local shear rate ($\dot{\gamma}$) based on the following models:

2.2.3.1 Power-law

$$\nu = k \dot{\gamma}^{n-1} \quad (3)$$

where,

- k is the consistency index
- n is the flow behaviour index ($n < 1$ shear-thinning, $n > 1$ shear-thickening, $n = 1$ Newtonian)

The Reynolds number for a power-law fluid is defined as:

$$Re_{PL} = \frac{\rho U^{2-n} L^n}{k} \quad (4)$$

where,

- ρ is the fluid density
- U is the characteristic velocity
- L is the characteristic length

2.2.3.2 Carreau model

$$\nu = \nu_{\infty} + (\nu_0 - \nu_{\infty}) \left[1 + (\lambda \dot{\gamma})^2 \right]^{\frac{n-1}{2}} \quad (5)$$

where,

- ν_0 and ν_{∞} are the zero and infinite-shear viscosities
- λ is the time constant
- n is the flow index

The dimensionless groups characterizing Carreau fluids are:

$$Re_C = \frac{\rho UL}{\mu_0}, \quad Cu = \frac{\lambda U}{L} \quad (6)$$

2.2.3.3 Carreau-Yasuda model

It extends the Carreau model with an additional parameter a to improve fitting:

$$\nu = \nu_{\infty} + (\nu_0 - \nu_{\infty}) \left[1 + (\lambda \dot{\gamma})^a \right]^{\frac{n-1}{a}} \quad (7)$$

where,

- a is the shape parameter that controls the width of the transition between the Newtonian plateau and the power-law regime

2.2.3.4 Casson model

$$\nu(\dot{\gamma}) = \left(\sqrt{\frac{\tau_0}{\dot{\gamma}}} + \sqrt{m} \right)^2 \quad (8)$$

where,

- τ_0 is the yield stress
- m is the consistency index

For Casson-type fluids, the relevant dimensionless groups are:

$$Re_{CA} = \frac{\rho UL}{\mu_{\infty}}, \quad Bn = \frac{\tau_0 L}{\mu_{\infty} U} \quad (9)$$

where,

- μ_{∞} is the asymptotic viscosity at high shear rates

3 Simulation Procedure

For the OpenFOAM simulations, the case directory is organized into 3 main folders: 0, constant, and system. The 0 folder defines the initial and boundary conditions for the flow variables, such as pressure (p) and velocity (U). The constant folder contains the mesh description under polyMesh and the fluid properties specified in transportProperties, including the parameters of the chosen viscosity model. The system folder includes files that govern the simulation setup, such as blockMeshDict for mesh generation, controlDict for run control, fvSchemes for discretization schemes, fvSolution for solver settings, and decomposeParDict for parallel execution. A summary of this folder structure for the nonNewtonianIcoFoam solver setup is provided in Table 1.

Table 1: Folder structure for simulation in OpenFOAM v2412

0/:
<p>p U</p>
constant/:
<p>polyMesh: boundary faces neighbour owner points transportProperties</p>
system/:
<p>blockMeshDict controlDict decomposeParDict fvSchemes fvSolution</p>

3.1 Geometry and Mesh

The geometry is as described in the problem definition with a thickness of 0.01 m extruded in z-direction. For meshing, uniform structured square blocks were generated without cell refinements applied in any direction. The nomenclature for boundary faces is as shown in Fig. 2.

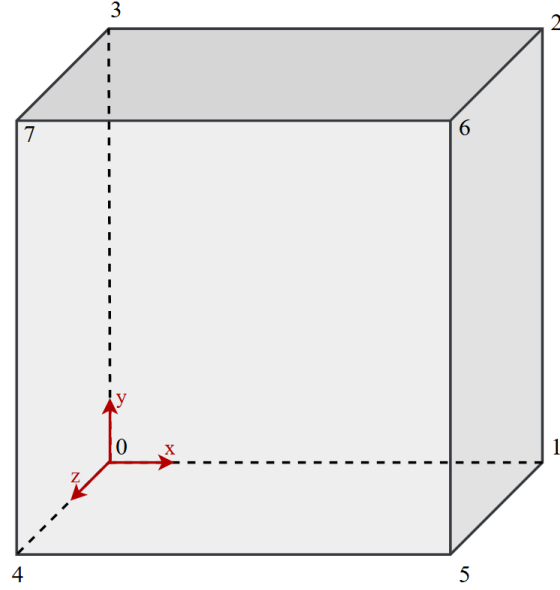


Figure 2: Block structure of mesh

3.2 Initial and Boundary Conditions

The initial and boundary conditions were assigned as shown in the Table 2.

Table 2: Boundary conditions for pressure and velocity.

Region	p (kg/m s ²)	U (m/s)
internalField	uniform 0	uniform (0 0 0)
movingWall	zeroGradient	uniform (1 0 0)
fixedWalls	zeroGradient	noSlip
frontAndBack	empty	empty

3.3 Solver

The nonNewtonianIcoFoam solver is an extension of the standard icoFoam solver in which the viscosity depends on the shear rate. It solves the incompressible Navier–Stokes equations using the finite volume method (FVM) and applies the PISO algorithm for pressure–velocity coupling, ensuring continuity equation is satisfied at each time step.

At each iteration, the viscosity is recalculated using the selected model. But compared to the Newtonian simulations, these repeated viscosity calculations raise the computational cost, particularly when small time steps and fine meshes are used. Furthermore, the solver is limited to laminar incompressible flows. Reliable results also depend heavily on the proper selection of viscosity models and their parameters.

4 Results and Discussions

4.1 Newtonian Validation

To verify the numerical methodology, the solver was first validated against the classical lid-driven cavity problem for Newtonian flow at $Re = 100$. It considered two standard parameters: (a) u -velocity along the vertical centerline and (b) v -velocity along the horizontal centerline. Figs.3a and 3b compare the present results with the benchmark data of Ghia et al. [5]. The velocity profiles match the reference data very well, which shows that the solver is accurate enough to work for non-Newtonian cases.

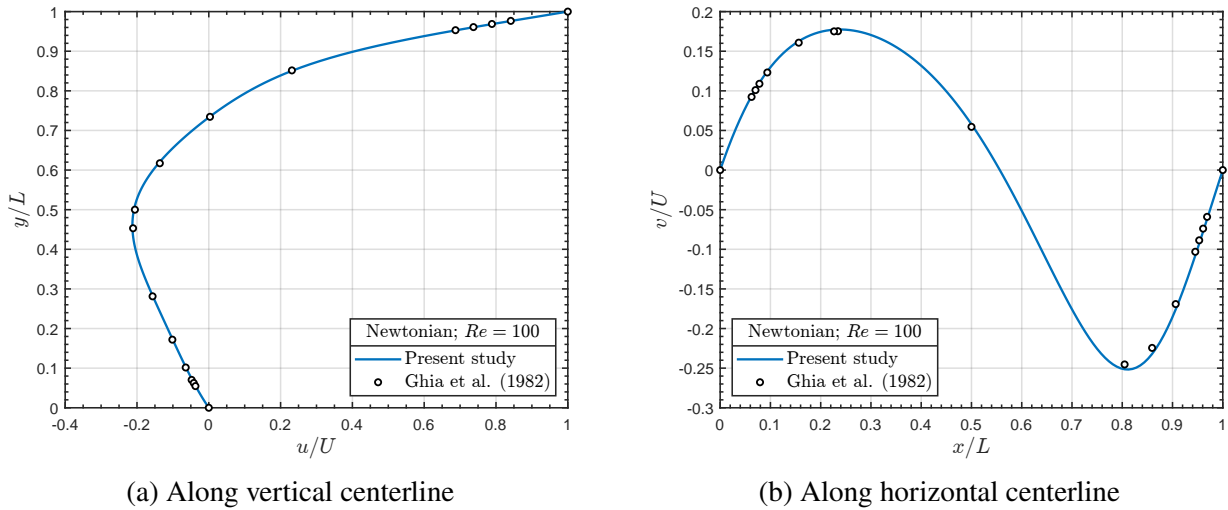


Figure 3: Normalised u and v -velocity profiles along cavity centerlines; Newtonian Model

4.2 Grid Independence Study

A grid independence study was performed for non-Newtonian fluid flow using the power-law model in the shear-thinning regime ($n = 0.5$) at $Re = 100$. Four uniform meshes (32×32 , 64×64 , 128×128 , and 256×256) were examined. The time step was chosen such that the Courant number remained below 0.5.

The pressure at the geometric centre of the cavity was monitored as the reference variable. Table 3 shows the center-point pressure values obtained for each mesh sizes, while Fig. 4 shows the convergence plot. It can be seen that the variation becomes very small beyond the 128×128 grid, indicating sufficient mesh resolution. Hence, the 128×128 mesh was adopted for all subsequent simulations as shown in Fig. 5.

4.3 Non-Newtonian Validation and Comparison with $Re = 400$

Figures 6–9 compare the normalised velocity profiles along the cavity centerlines for all four non-Newtonian models at $Re = 100$ and $Re = 400$. Subfigure (a) shows the u -velocity along the vertical centerline, while subfigure (b) shows the v -velocity along the horizontal centerline. At $Re = 100$,

Table 3: Effect of mesh resolution on center-point pressure (Power-law model, $n = 0.5$).

Mesh Size	Total Cells	p at Centre (Pa)
32×32	1,024	-0.00334272
64×64	4,096	-0.00419802
128×128	16,384	-0.00483776
256×256	65,536	-0.00530957

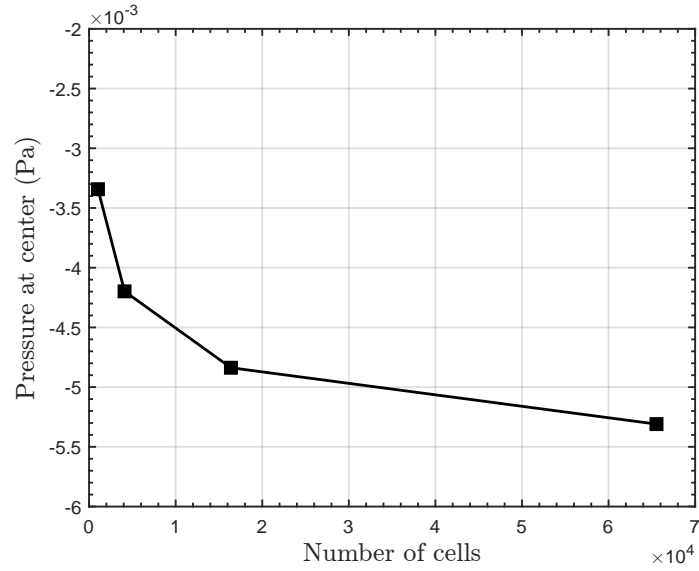
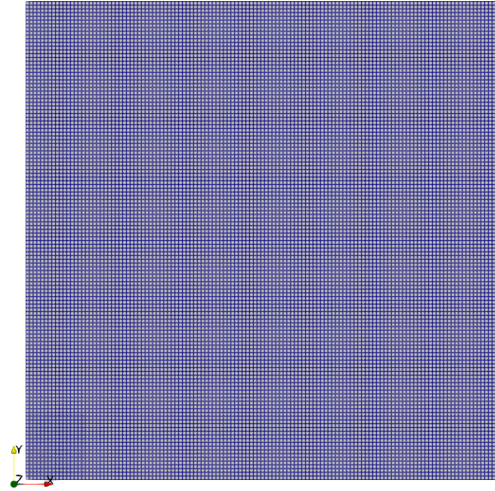


Figure 4: Grid convergence plot

Figure 5: 128×128 mesh

the results for each viscosity model agree well with benchmark data from the literature, confirming the accuracy of the present solver setup.

4.3.1 Power-law Model

The simulation was conducted for both shear-thinning ($n = 0.5$) and shear-thickening ($n = 1.5$) cases. As seen in Fig. 6, the u -velocity shows that higher n gives steeper gradients near the lid and bottom wall. This is because shear-thickening fluids ($n > 1$) increase viscosity in high-shear regions. The v -velocity becomes sharper with higher peaks as n increases.

At $Re = 400$, both velocity profiles show steeper gradients and larger peaks, with extrema shifting toward the walls. This agrees with Li *et al.* [1], which showed that higher Re increases circulation and highlights the differences between shear-thinning and shear-thickening flows.

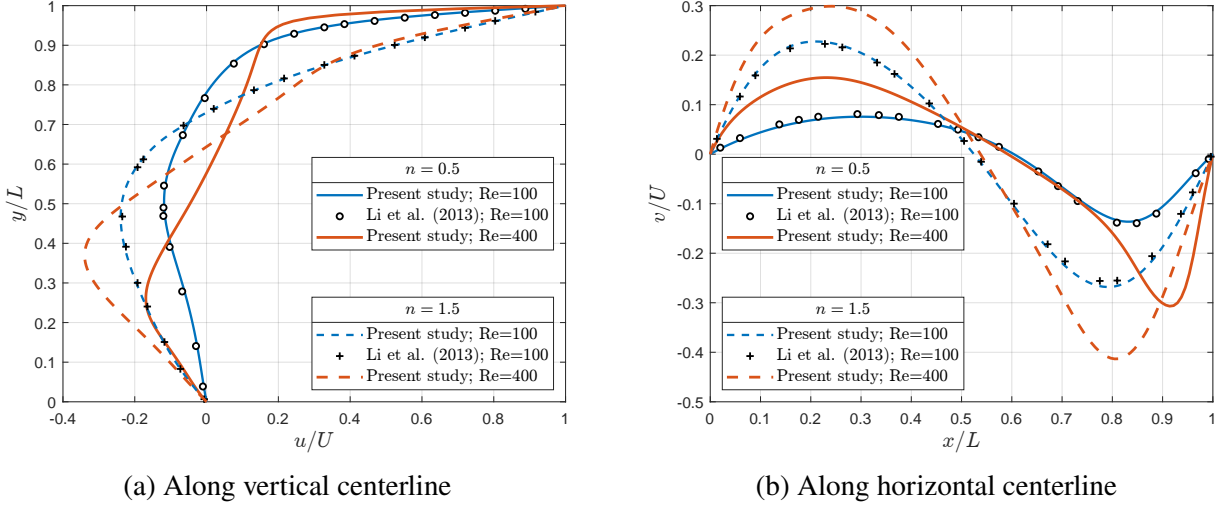


Figure 6: Normalised u and v -velocity profiles along cavity centerlines; Power-law Model

4.3.2 Carreau Model

The Carreau fluid is considered with $n = 0.5$, $\lambda = 1$, $\mu_0/\mu_\infty = 100$, and $Cu = 1$, using parameters from Kim and Reddy [2]. At $Re = 100$, the u -velocity increases smoothly with steep gradients near the lid, while the v -velocity follows a sinusoidal shape with moderate peaks as seen in Fig. 7.

At $Re = 400$, the u -velocity slope near the lid becomes sharper and the v -velocity extrema shift closer to the walls, showing stronger inertial effects and shear-thinning behavior.

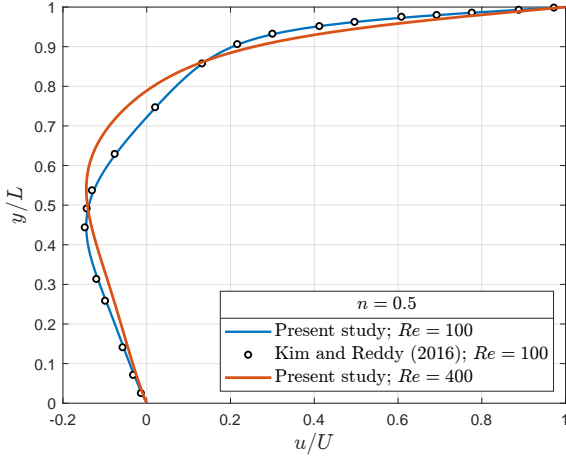
4.3.3 Carreau–Yasuda Model

The Carreau–Yasuda fluid is considered with $n = 0.5$, $a = 0.2$, $\lambda = 1$, and $\mu_0/\mu_\infty = 100$, using parameters from Kim and Reddy [2]. At $Re = 100$, the velocity profiles are broader than in the Carreau case, with smoother gradients and a more gradual sinusoidal variation in v -velocity.

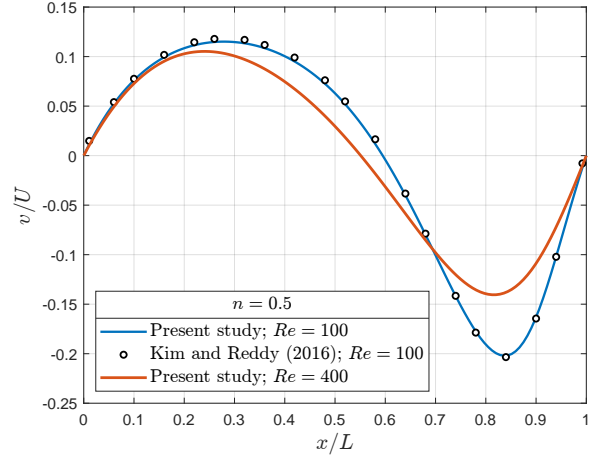
At $Re = 400$, near-lid gradients become steeper and v -velocity extrema intensify, but the broader profiles remain, giving smoother circulation compared to the Carreau model.

4.3.4 Casson Model

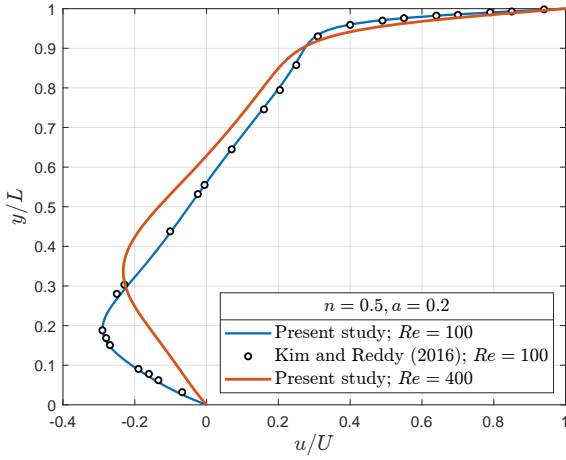
The Casson model is tested with $Bn = 0.1$ and $Re = 100$, corresponding to a yield stress $\tau_0 = 0.001$. The velocity profiles match well with Neofytou [3] and appear flatter in the cavity center than shear-



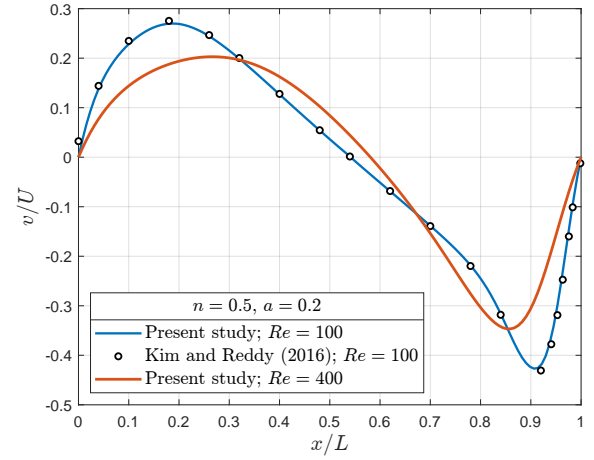
(a) Along vertical centerline



(b) Along horizontal centerline

Figure 7: Normalised u and v -velocity profiles along cavity centerlines; Carreau Model

(a) Along vertical centerline



(b) Along horizontal centerline

Figure 8: Normalised u and v -velocity profiles along cavity centerlines; Carreau-Yasuda Model

thinning cases, as the yield stress reduces motion in low-shear regions.

At $Re = 400$, the yield-stress effect is still present, but stronger lid motion increases near-wall gradients and shifts the velocity extrema toward the cavity center.

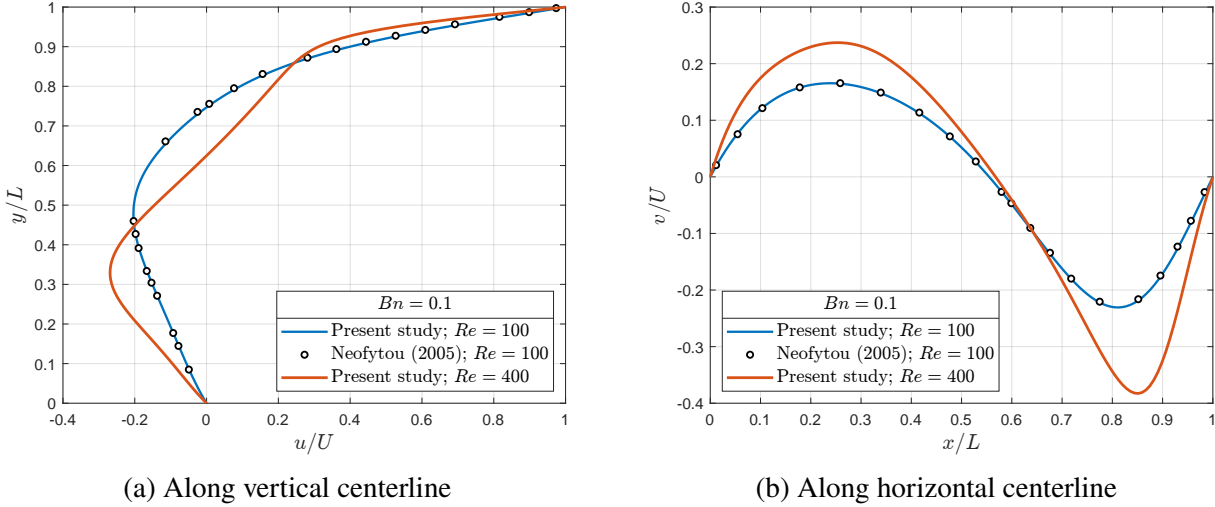


Figure 9: Normalised u and v -velocity profiles along cavity centerlines; Casson Model

5 Conclusion

In this study, the `nonNewtonianIcoFoam` solver in OpenFOAM was used to study transient simulations of two-dimensional lid-driven cavity flows for non-Newtonian fluids. The Power-law, Carreau, Carreau–Yasuda, and Casson viscosity models were taken into consideration. Shear-thinning, shear-thickening, and yield-stress characteristics were captured by the solver, which reproduced velocity profiles in close agreement with the benchmark data.

A grid independence study confirmed that a 128×128 mesh was adequate for the present cases. Shear-thinning fluids produced smoother gradients, while shear-thickening fluids showed steeper slopes and more distinct v -velocity peaks. The Carreau and Carreau–Yasuda models both represented shear-thinning behavior, with the Carreau–Yasuda model yielding broader and smoother transitions at higher Reynolds numbers. The Casson model emphasized yield-stress effects, flattening centerline profiles, and reducing motion in low-shear regions. Increasing Reynolds number from 100 to 400 consistently sharpened near-wall gradients, strengthened circulation, and shifted velocity extrema toward the walls.

These results indicate that open-source CFD softwares, such as OpenFOAM can effectively capture the key features of non-Newtonian cavity flows, providing a reliable framework for rheological flow studies.

6 Acknowledgements

I would like to express my sincere gratitude to my supervisors, Dr. Tushar Chourushi and Dr. Chandan Bose, for their continuous guidance and invaluable insights throughout the project. This work would not have been possible without their patient support and constructive feedback at every stage.

I am also grateful to Ms. Payel Mukherjee, Project Manager at FOSSEE and to the entire FOSSEE team for their support and for providing me with the opportunity to learn, explore and contribute.

References

- [1] Q. Li, N. Hong, B. Shi, and Z. Chai, “Simulation of Power-Law fluid flows in Two-Dimensional square cavity using Multi-Relaxation-Time Lattice Boltzmann method,” *Communications in Computational Physics*, vol. 15, no. 1, pp. 265–284, 8 2013. [Online]. Available: <https://doi.org/10.4208/cicp.160212.210513a>
- [2] N. Kim and J. N. Reddy, “A spectral/hp least-squares finite element analysis of the Carreau–Yasuda fluids,” *International Journal for Numerical Methods in Fluids*, vol. 82, no. 9, pp. 541–566, 2 2016. [Online]. Available: <https://doi.org/10.1002/fld.4230>
- [3] P. Neofytou, “A 3rd order upwind finite volume method for generalised Newtonian fluid flows,” *Advances in Engineering Software*, vol. 36, no. 10, pp. 664–680, 5 2005. [Online]. Available: <https://doi.org/10.1016/j.advengsoft.2005.03.011>
- [4] M. Bisht and D. V. Patil, “Assessment of multiple relaxation time-lattice Boltzmann method framework for non-Newtonian fluid flow simulations,” *European Journal of Mechanics - B/Fluids*, vol. 85, pp. 322–334, 10 2021. [Online]. Available: <https://doi.org/10.1016/j.euromechflu.2020.10.005>
- [5] U. Ghia, K. Ghia, and C. Shin, “High-Re solutions for incompressible flow using the Navier-Stokes equations and a multigrid method,” *Journal of Computational Physics*, vol. 48, no. 3, pp. 387–411, 12 1982. [Online]. Available: [https://doi.org/10.1016/0021-9991\(82\)90058-4](https://doi.org/10.1016/0021-9991(82)90058-4)